JOURNAL OF MAGNETIC RESONANCE **133,** 304–312 (1998)
ARTICLE NO. MN981476

Application of the Filter Diagonalization Method to One- and Two-Dimensional NMR Spectra

Vladimir A. Mandelshtam,* Howard S. Taylor,† and A. J. Shaka*,[1]

*Chemistry Department, University of California, Irvine, California 92697-2025; and †Chemistry Department, University of Southern California, Los Angeles, California 90089

Received September 24, 1997; revised April 16, 1998

A new non-Fourier data processing algorithm, the filter diagonalization method (FDM), is presented and applied to phase-sensitive 1D and 2D NMR spectra. FDM extracts parameters (peak positions, linewidths, amplitudes, and phases) directly from the time-domain data by fitting the data to a sum of damped complex sinusoids. Grounded in a quantum-mechanical formalism, FDM shares some of the features of linear prediction and other linear algebraic approaches, but is numerically more efficient, scaling like the fast Fourier transform algorithm with respect to data size, and has the ability to correctly handle spectra with thousands or even millions of lines where the competing methods break down. Results obtained on complex spectra are promising.

Key Words: **filter diagonalization method (FDM); linear prediction; 2D NMR data processing; *J* spectroscopy; phase-twist lineshape.**

INTRODUCTION

NMR spectra can be subject to a variety of known imperfections. For example, the first few data points of the free induction decay (FID) can be corrupted by the risetime of the audio filters, the ringdown of the probe after a pulse, or hardware delays before the beginning of acquisition necessary, for example, to reestablish magnetic field homogeneity and stability after the application of a pulsed field gradient (PFG). In two-dimensional (2D) NMR it may not be possible to acquire a sufficiently long signal to obtain the desired resolution in the interferometric or F_1 dimension because each t_1 increment requires at least one repetition of the entire pulse sequence and acquisition, and the sensitivity of the 2D experiment can decrease markedly if the maximum acquisition time in F_1, $t_{1\max}$, becomes long, necessitating extensive time averaging to obtain an acceptable signal-to-noise ratio in the final spectrum (*1*). Finally, in some cases, the lineshape after 2D Fourier transformation (FT) is intrinsically undesirable. It is well known that spectra which are purely phase modulated as a function of t_1 give rise to mixed-phase (''phase-twist'') lineshapes in which neither the real nor the imaginary part of the 2DFT spectrum can be phased to the desired double absorption lineshape (*2*). A perfect example of this phenomenon occurs in 2D *J*-resolved spectroscopy (*3*), in which the phase-twist lineshape both distorts proton multiplet cross sections and necessitates an absolute-value 45° integral projection when trying to obtain a homonuclear decoupled proton spectrum. The long tails of the dispersion-mode lineshape dominate the absolute-value projection, leading to disappointing resolution in the decoupled spectrum.

In this article we demonstrate an alternative method to standard FT analysis called the filter diagonalization method (FDM). As we will show, FDM is related to existing linear algebraic methods but has important practical advantages computationally with regard to speed, stability, the ability to efficiently process very long time signals with many (e.g., 10^6) spectral features, and the ability to process multidimensional signals directly. The output of FDM is a ''line list'' of spectral parameters for Lorentzian lines in terms of frequency, width, amplitude, and phase. This direct representation of the spectral parameters can be obtained, even for very large 2D data sets, with perfectly acceptable computation times on readily available computers, and it is in this arena that FDM shines. Compared to processing and phasing an FT spectrum, and then obtaining a ''line listing'' by analyzing the spectral features, FDM appears to be more efficient, can offer better resolution in the case of truncated signals, and gives the possibility of immediate data compression. In addition, the direct representation of the data makes it possible to manipulate unfavorable 2D lineshapes like the phase twist into pure double absorption-mode lineshapes.

The FDM line list can be used to create a substitute or ''ersatz'' NMR spectrum. This is, from an experimentalist's viewpoint, an aggressive approach, in which any signal not detected by FDM will vanish from the spectrum. The justification for this approach will hinge on comparison of the ersatz spectrum with the FFT spectrum in cases where the data set is known to be complete. An alternative and more conservative approach is to calculate a ''hybrid'' spectrum by (i) constructing the ersatz spectrum; (ii) synthesizing the time-domain signal corresponding to this spectrum; (iii) subtracting this

[1] To whom correspondence should be addressed. ajshaka@uci.edu.

1090-7807/98 $25.00

signal from the original data; and (iv) Fourier transforming this residual time signal, adding the result to the ersatz spectrum. This hybrid approach is more conservative in that the original noise, etc., in the data is retained but in which there may be substantial improvement in spectral lineshapes. The relationship of these spectra to previous approaches will become clear in what follows.

THEORY

The Filter Diagonalization Method

FDM was first introduced in 1995 by Wall and Neuhauser (*4*) as a method of spectral analysis of (one-dimensional) time correlation functions in quantum dynamics calculations. It has subsequently been substantially improved (*5, 6*) and extended to the case of the multidimensional model (*7*) and experimental (*8*) time signals. FDM has also been applied to a number of important problems in the fields of theoretical chemistry and physics (*9–13*) where it has shown both conceptual simplicity and numerical efficiency when compared to past methods, and where it has been accepted with enthusiasm. As the main point of this paper is the actual experimental results we have obtained using FDM with optimized pulse sequences, we will only summarize the basic ideas and sketch the mathematical underpinnings, without repeating detailed formulas. A detailed account of 1D FDM (*14*) and 2D FDM (*8*) theory as applied to time-domain NMR signals has already been given.

FDM is designed to solve the *harmonic inversion problem*, which is essentially that of fitting the given complex time signal $c_n = C(t_n)$ defined on an equidistant time grid $t_n = n\tau$, $n = 0, 1, \ldots, N$, to the sum of exponentially damped sinusoids,

$$c_n = \sum_{k=1}^{K} d_k \exp(-in\tau\omega_k), \qquad [1]$$

with a total of $2K$ unknowns, the K complex amplitudes d_k, and the K complex frequencies $\omega_k = 2\pi f_k - i\gamma_k$, which include the damping. The more compact notation ω_k is preferred, as the imaginary parts γ_k (widths) of the frequencies always appear together with the real parts $2\pi f_k$ (positions) in FDM. Even though the harmonic inversion problem is highly nonlinear, its solution can be obtained purely by linear algebraic methods, of which there are many variants. Some, like the Prony method (*15*), MUSIC (*16*), ESPRIT (*17*), etc., are well known in signal processing circles in the electrical engineering literature, and others, like linear prediction (LP), have already been used extensively in NMR applications (*18–25*) and are mature enough that entire books have been devoted to their exposition (*26*). There are some important differences between these alternatives, some of which hinge on whether there may be any prior knowledge about the signal in question. FDM makes no assumptions concerning the number of lines, their frequencies, or the level of noise contaminating the desired signal.

Briefly, the central ansatz (assumption) of FDM is to associate the signal c_n to be fitted by the form of Eq. [1] with the time autocorrelation function of a fictitious dynamical system described by an effective complex symmetric Hamiltonian operator $\hat{\Omega}$ with eigenvalues $\{\omega_k\}$ (*4*)

$$c_n = (\Phi_0 \mid e^{-in\tau\hat{\Omega}}\Phi_0) \qquad [2]$$

on some ''initial state'' Φ_0. The notation (.|.) denotes a complex symmetric inner product, $(a|b) = (b|a)$, without complex conjugation. Note that under the assumption that $\hat{\Omega}$ has a finite rank, the usual LP formulas can be derived from Eq. [2]. However, FDM does not require $\hat{\Omega}$ to be of finite rank. Using Eq. [2], the fitting problem becomes equivalent to diagonalizing $\hat{\Omega}$ or, equivalently (*6*), the evolution operator over a single time step $\hat{U} = \exp(-i\tau\hat{\Omega})$. Although we do not know either $\hat{U}$ or Φ_0, we can still find a basis in which matrix representations of $\hat{U}$ can be constructed. Furthermore, by a clever choice of basis, it is possible to make the matrix representation of $\hat{U}$ (i) completely determined by the measured signal c_n; (ii) diagonally dominant, with off-diagonal matrix elements that tend to decay with a roughly sinc-like dependence along the minor diagonal; and (iii) ordered according to frequency, just like the conventional NMR spectrum. This matrix is easy to diagonalize, and can be handled in series of frequency windows, each of which generates a small submatrix of size $K_{\mathrm{win}} \times K_{\mathrm{win}}$, where K_{win} is between 3 and 100 depending on the details of the problem. Finally, because an FFT can be used to construct the matrix elements of $\hat{U}$ from the FID itself (*14*) the numerical effort to construct these matrices scales like the FFT, namely roughly $N \log N$ for an FID of N complex points.

A general *two-dimensional* harmonic inversion problem can be formulated as a nonlinear fit of a 2D time-domain array c_{n_1,n_2} by the plane wave representation

$$c_{n_1,n_2} = \sum_{k=1}^{K} d_k \exp(-in_1\tau_1\omega_{1k})\exp(-in_2\tau_2\omega_{2k}) \qquad [3]$$

with a total of $3K$ unknown complex numbers, i.e., the K complex amplitudes d_k and two sets of K complex frequencies $(\omega_{1k}, \omega_{2k})$. The key ansatz of 2D FDM is obtained by introducing two commuting complex symmetric operators $\hat{\Omega}_1$, $\hat{\Omega}_2$, having the same set of eigenvectors Y_k but different eigenvalues ω_{1k}, and ω_{2k} which are the unknown complex frequencies:

$$c_{n_1,n_2} = (\Phi_0 | e^{-in_1\hat{\Omega}_1\tau_1} e^{-in_2\hat{\Omega}_2\tau_2}\Phi_0). \qquad [4]$$

Diagonalization of the operators $\hat{U}_1 = \exp(-in\hat{\Omega}_1\tau_1)$ and $\hat{U}_2 = \exp(-in\hat{\Omega}_2\tau_2)$ then yields the desired frequency coordinates (and widths) ω_{1k}, and ω_{2k} of the peak in the two-dimensional

plane, while the eigenvector Y_k yields the intensity and phase, d_k (*7*, *8*).

Spectral Representations: Ersatz Spectra

Assuming that the spectral parameters can be estimated by FDM, an ''ersatz spectrum'' can easily be constructed by summing over these parameters. As such the 1D absorption ersatz spectrum of the (real) running frequency F is given by

$$A(F) = -\sum_k \mathrm{Im}\left\{\frac{d_k}{2\pi F - \omega_k}\right\}. \quad [5]$$

Since, in the language of complex analysis, the spectrum is determined by the position of ω_k, in the complex plane, it is economical to refer to each entry in the line list as a *pole.* Another useful example is the absorption-mode part of a 2D ersatz spectrum, which can be defined as a function of the real frequencies F_1, F_2 as, e.g.,

$$A(F_1, F_2) = \sum_k \mathrm{Im}\left\{\frac{1}{2\pi F_1 - \omega_{1k}}\right\}\mathrm{Im}\left\{\frac{d_k}{2\pi F_2 - \omega_{2k}}\right\}, \quad [6]$$

in which it is assumed that the features are all in phase in F_1. Note here that while the quantity $A(F_1, F_2)$ is obtained trivially in terms of the spectral parameters, the expression in Eq. [6] is highly nonlinear. In fact, there is some freedom in how one chooses to construct a spectrum from the FDM line list. It is always possible to construct a spectrum which would agree with the conventional 2D FT spectrum, although this avenue is unlikely to be useful if the 2D lineshapes are phase twists. While the FDM line list itself may be of most use for other computer programs to exploit, for example, in database searching or automated assignment procedures, spectral representations are more useful for human appraisal.

Informational Considerations in 2D FDM

Clearly, the methods of spectral analysis based on solution of the harmonic inversion problem, Eqs. [1] and [3], are conceptually different from those based on the FT. In particular, the time-frequency ''uncertainty principle,''

$$\delta\omega = 2\pi/N\tau, \quad [7]$$

which is an intrinsic property of the FT, can be sidestepped by solving the harmonic inversion problem: the spectral resolution δf, defined by the width of a single peak or by the distance between two close peaks, can be very small because the complex frequencies ω_k are now simply the fitting parameters. The quality of the fit is determined partly by signal-to-noise considerations and can be very high even for short data records. This difference becomes even more striking when the multidimensional harmonic inversion problem, Eq. [3], is compared to a conventional 2DFT spectral analysis. In the latter case the uncertainty principle is applied to each dimension *separately*, requiring a sufficiently long extension of the 2D signal c_{n_1,n_2} in both directions, n_1 and n_2. When a fitting problem is to be solved the requirement for the size, N_1, N_2, of the 2D signal is not that strict. From the informational point of view, all unknown spectral parameters (d_k, ω_{1k}, ω_{2k}) can be extracted to a precision dictated by signal-to-noise considerations once the total amount of data, the product N_1N_2, is greater than the total number of unknowns, $3K$. This means that, in some cases, it may be possible to ''make up'' for poor sampling along one dimension by increasing the sampling along a *different* dimension, which would be very attractive for some NMR applications, in which it is typically easy to obtain good digitization in F_2. This statement is strictly true for a model signal of randomly distributed narrow lines in the 2D plane (*7*) and is approximately true for real 2D NMR data in the absence of wide lines, many peaks with degenerate frequencies in either of the two dimensions, and t_1 noise. Other possible limitations include true noise, and numerical limitations associated with the highly nonlinear character of the harmonic inversion problem. This potential advantage is discarded once a Fourier transform is performed in the F_2 dimension, as is normally done in NMR applications using LP, because then each interferogram is treated separately, ignoring important correlations which are picked up by an up-front 2D method.

It is important to realize the difference between the present formulation of the 2D harmonic inversion problem, Eq. [3], which consists of a *single sum* over intrinsically 2D features, and the direct-product formulations proposed previously in the context of LP (*27–29*). In the latter case the authors used models with a direct-product set of unknown spectral parameters, $\{\omega_{1k}, \omega_{2k'}, d_{kk'}\}$, $k = 1, 2, \ldots, K_1$, $k' = 1, 2, \ldots, K_2$, so that in the 2D plane the unknown spectral features would form a rectangular $K_1 \times K_2$ grid with total $K_1 + K_2 + K_1^*K_2$ number of unknown parameters. In Eq. [3] the 2D frequencies ω_{1k}, ω_{2k} need *not* form a direct-product 2D grid. The present non-direct-product model does not preclude a direct-product output (as, e.g., in the case of COSY and NOESY) yet results in a much more compact representation for cases when the 2D spectra do not have direct-product patterns, for example, HSQC or 2D J spectra, which are anticipated to be the most suitable applications for the present technique.

Local Spectral Analysis

Even though the harmonic inversion problem is a highly nonlinear one, its solution, as in FDM, can be obtained by pure linear algebra. This feature is shared by the other ''high-resolution'' methods (*15–26*). What makes FDM different from most of the other linear algebraic approaches,

and thereby makes it far more useful for multidimensional NMR applications, is its ability to avoid dealing with a large linear algebraic problem of size at least as large as the rank K of the signal subspace, which must include noise. This is done by performing the spectral analysis locally for a chosen frequency domain and, consequently, by solving a small eigenvalue problem whose eigenvalues and eigenvectors then yield the desired complex frequencies (ω_{1k}, ω_{2k}) and amplitudes d_k in this small spectral region. This ability to hone in and perform a local spectral analysis thus avoids problems of estimating the total rank K of the signal subspace. The parameters obtained are insensitive to spectral properties outside the chosen small spectral domain, as may be shown by adjusting the size of the latter and finding identical results (*6–8*).

This divide-and-conquer strategy breaks down the harmonic inversion problem, given by Eq. [1] or [3], into a series of small spectral domains, each of which is handled in a numerically stable, speedy, and reliable fashion. A comment should be made here as the latter statement seems to be in conflict with the harmonic inversion problem, which implies a global fit of the entire time-domain signal, and as the problem of choosing the parameter K is known to be a major difficulty in the other linear algebraic approaches based on the *global* fit of the signal by the sum of sinusoids. It is known, for example, that a large filter length K should be used in LP analysis whenever noise is present (*26*), yet for long FIDs even a 1D problem produces matrices which take days to handle on a vector computer (*24*) so the tendency is to skimp somewhat on K, using the smallest value that works. In FDM, however, no attempt is made to achieve a global fit in one shot. The size K_{win} of the small generalized eigenvalue problem is, in principle, an adjustable parameter, just like K. For a given K_{win} not more than K_{win} complex poles ω_k can be extracted: some of these poles may be the true signal poles, and some may represent noise. Based on our experience and the informational considerations (*7*), however, *we never consider* K_{win} *as an adjustable parameter,* but instead, over a spectral region $[F_{\min}, F_{\max}]$ in a spectrum of spectral width SW, use the fixed formula

$$K_{\text{win}} = \varkappa \frac{N}{2} \frac{(F_{\max} - F_{\min})}{\text{SW}}, \qquad [8]$$

that is, the largest number possible consistent with the local information content of the signal. The factor $\varkappa$ is between 1.0 and 1.1 to take account of edge effects. For a sufficiently long FID, $\varkappa$ is fixed at 1.0. When truncation is significant, so that the grid points may be quite sparse, $\varkappa$ is fixed at 1.1. Whenever the fit is excellent it is also insensitive to $\varkappa$. When all is said and done, FDM thus uses the *maximum number of poles* to fit the entire frequency range, namely $N/2$ for an FID of length N complex points. This is important to realize when comparing the timing of FDM with LP methods, as in the latter the filter length is usually chosen to be somewhat shorter than $N/2$. An analogous 2D formula is used for 2D spectral domains $[F_{1\min}, F_{1\max}] \times [F_{2\min}, F_{2\max}]$.

A conceptually similar but numerically different technique, LP-ZOOM, is a modification of the linear prediction algorithm for local spectral analysis, and was demonstrated in 1988 (*30*). LP-ZOOM potentially shares many of the advantages of FDM but uses the familiar LP procedure to construct the LP coefficients using a chosen filter length and determines the frequencies and widths, and then the amplitudes and phases, so that there are more adjustable parameters to optimize. LP-ZOOM is far preferable to conventional LP methods, but no 2D formulation of LP-ZOOM is available in the sense of Eq. [3].

Numerical Efficiency

There are two parts to the FDM algorithm, the construction of the matrices $\hat{U}$ and their diagonalization. Assuming that the diagonalization scales as K_{win}^3, the total numerical effort to extract the spectral parameters will scale as $N \log N + (N/2K_{\text{win}})K_{\text{win}}^3$. The first term assumes that the matrix elements are obtained by an FFT algorithm, and the second just counts the number of frequency windows that need to be used. In practice, for most NMR signals, the diagonalization portion takes the lion's share of the CPU time. As such, using the FFT algorithm is not strictly necessary. Note, however, that for reasonable values of N the scaling is actually purely linear as far as the diagonalization portion is concerned, as K_{win} can remain fixed. In addition, due to the small size of the matrices involved, FDM does not encounter numerical problems caused by the ill-conditioned nature of these matrices; nor does it suffer from the typical K^3 scaling of the numerical effort with respect to the rank of the signal subspace that is characteristic of conventional LP methods. Finally, it is possible to implement FDM trivially on a parallel architecture computer by simply assigning each processor its own spectral domain to analyze. These features, and the fact that in some NMR experiments one has a rather good idea of where to expect signals or what signals

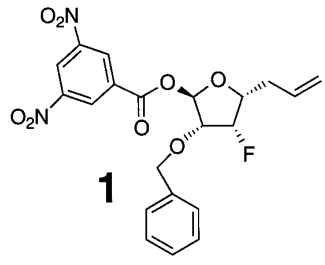

FIG. 1. The molecule under study. The resonances shown in the NMR spectra in Fig. 2 arise from the protons on the ribose ring and several of the substituents. Spin–spin coupling to fluorine-19 creates extra splittings in the spectrum.

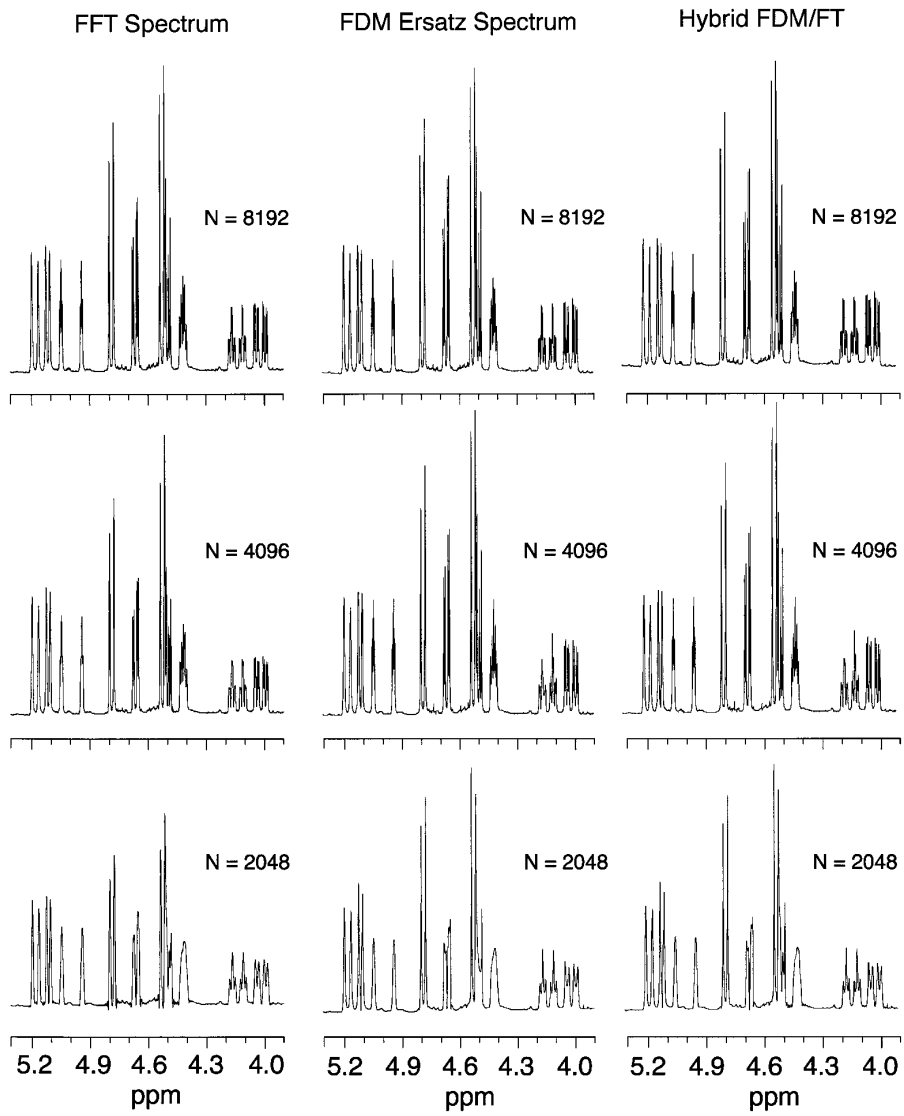

FIG. 2. A 1.4 ppm section of the 1D spectrum of **1** obtained by various data processing methods. The three FT spectra on the left show the quality of the data and change in lineshape and resolution when the signal is truncated. Digital filtering and zero-filling have been used to obtain the best spectral representation. The central three spectra are ersatz spectra constructed artificially from the poles of Eq. [2] detected by FDM. Although not easily visible at the vertical scale of the figure, very small peaks in the baseline were identified with fidelity by FDM. The convergence onto the spectral features is somewhat different than with the FT spectra. Note that narrow spectral features, especially if relatively isolated, are located very accurately. Wide overlapping lines converge onto the correct amplitudes and widths more slowly with respect to the number of time-domain points. As follows from Eq. [8], a total of 264, 132, and 66 poles were used to construct the ersatz spectra for the cases $N = 8192$, 4096, and 2048, respectively, in an ~1.4 ppm region centered on the expansion shown. Note, however, that far fewer than this number of poles have significantly large amplitudes d_k. The far right column shows the hybrid spectrum obtained as described in the text.

are of particular interest, make FDM potentially extremely useful in high-resolution NMR.

EXPERIMENTAL

Having emphasized the main features of FDM we now demonstrate it on the experimental NMR signals and compare the results with those obtained by conventional FT-based spectral analysis. To demonstrate the actual power of the method we chose quite long signals ($N_2 \sim 10^4$) having quite complex spectra, so that efficient applications of the other linear algebraic methods would be questionable. All proton NMR spectra were obtained at 25°C on a 500-MHz Varian UnityPlus spectrometer equipped with a Varian triple-resonance pulsed field gradient probe. Precautions were taken to shim the magnet to obtain good, but not outstanding, lineshape. There was no special sample preparation. Processing was accomplished off-line on a small SGI Indigo workstation or on a Pentium 133-MHz PC. It actually took sig-

nificantly more time to convert the data from one format to another than to process it with FDM.

1D FDM

First we test the 1D version of FDM on a representative section of the 1D NMR spectrum of the molecule shown in Fig. 1, a fluorinated ribose derivative. A 1.6 ppm interesting section of the spectrum was selected, and the central 1.4 ppm section is shown in Fig. 2 under a variety of processing conditions. As is typical of many reaction product mixtures, traces of impurity peaks are evident in the baseline. A large spin–spin coupling to ^{19}F has split some of the proton multiplets. At top left is the conventional FT spectrum obtained in 16 scans using 8K complex points over a spectral width of 10 kHz, with the 700-Hz region of interest plotted. The spectra directly below show the effect of truncating the time-domain signal at the indicated number of data points. Apodization, to avoid severe truncation effects, and zero-filling have been employed throughout. As more and more of the FID is deleted, the frequency resolution is degraded, in accordance with expectation. The three panels in the middle column show the FDM ersatz spectra, constructed from the poles isolated by FDM using Eq. [2], from the same FID. We must emphasize that these spectra are obtained *directly* from the time-domain data itself, and not by any ''extension'' of the truncated FID followed by a conventional FT, as is many times done with the LP method. The right traces show the hybrid spectrum described earlier, in which the residual between the original data and the FDM fit is Fourier transformed and added to the ersatz spectrum. For the complete signal, along the top row, there is negligible difference between the ersatz spectrum and the hybrid spectrum, showing that FDM can achieve an excellent fit. The hybrid spectrum is similar in spirit to that obtained by extension of an FID with LP followed by a conventional FT. However, LP extension and conventional FT is a slight modification of FT analysis. The hybrid spectrum is, on the other hand, a slight modification of FDM, as it is FDM that was used to construct the spectral features. To the extent that narrow spectral features are correctly identified by FDM, these lines are completely subtracted from the time-domain data, and so the truncation artifacts that would have been produced by the FT are avoided. The advantage of the hybrid spectrum is that it retains noise, baseline roll, and other features of the recorded data, and so is a conservative approach. The disadvantage is that certain limitations of the FT itself cannot be overcome in the hybrid spectrum, although if the residual is fairly small the FT limitations apply only to an insignificant part of the data.

With regard to the numerical effort to obtain the ersatz spectra shown, the total CPU time on a Pentium 133-MHz PC using an unoptimized FORTRAN code compiled with the free *gnu* compiler under LINUX were 5, 13, and 32 s for the 2048, 4096, and 8192 data sets, respectively. The scaling is not strictly linear because this code uses a *slow* FT to construct the matrix elements, and K_{win} was allowed to vary somewhat, for convenience. If the entire spectral width were processed, these times would increase by a factor of about 14. Note, however, that it is not necessary to process empty spectral regions, or regions of little interest, like those around a residual solvent resonance.

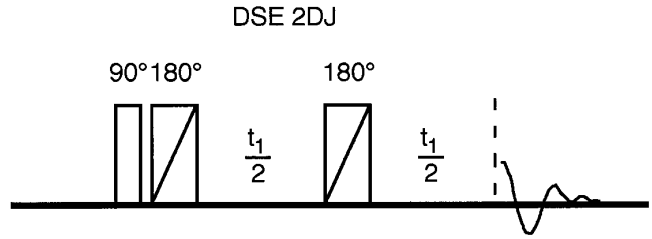

FIG. 3. A modified pulse sequence for 2D *J*-resolved spectroscopy using a double spin echo (DSE). The 180° inversion pulses were 50-μs FM pulses with a constant 25-kHz RF amplitude designed to invert the entire proton bandwidth. Phase shifts of the spin echo which would be created by the application of a single such pulse are conveniently removed by a second inversion pulse immediately after the 90° excitation pulse.

2D FDM

The 2D *J*-resolved spectrum of the same molecule was obtained using the pulse sequence of Fig. 3. This pulse sequence differs slightly from the conventional 2D *J* sequence in that two inversion pulses are used, one directly after the 90° excitation pulse. This double spin echo (DSE) allows one to use highly efficient frequency-modulated (FM) inversion pulses without any offset-dependent or B_1-dependent phase shifts, as the even-numbered echoes from any composite inversion pulse have constant phase (*31*). The use of a very accurate 180° pulse makes certain that coherence transfer processes akin to those in a COSY spectrum do not occur, minimizing artifacts in the 2D *J*-resolved spectrum.

The top trace in Fig. 4 shows an integral projection of the absolute-value 2D *J* spectrum along the 45° diagonal in frequency space, to give the proton–proton decoupled spectrum of the same 1.6 ppm region. Coupling to fluorine-19 is not, of course, removed in the projection. The data matrix consisted of 16K complex points over a 10-kHz spectral width in F_2, zero-filled to 32K, and 64 increments in F_1 over a spectral width of ± 50 Hz, zero-filled to 128 points. Digital resolution is thus quite good but, as is well known, the dispersion-mode tails of the phase-twist lineshape lead to ''Eiffel Tower'' lineshapes in the projection, in which the decoupled line is far wider than an individual multiplet line in the absorption-mode 1D spectrum. Various remedies have been tried in the past. The use of heavy resolution enhancement digital filters like the ''pseudo-echo'' can improve the appearance of the projection, but at the cost of large intensity distortions between lines of different natural linewidth, and a heavy toll in sensitivity (*32*). Frequency-domain computer procedures to iteratively remove the dispersion-mode contributions, and so avoid the null pro-

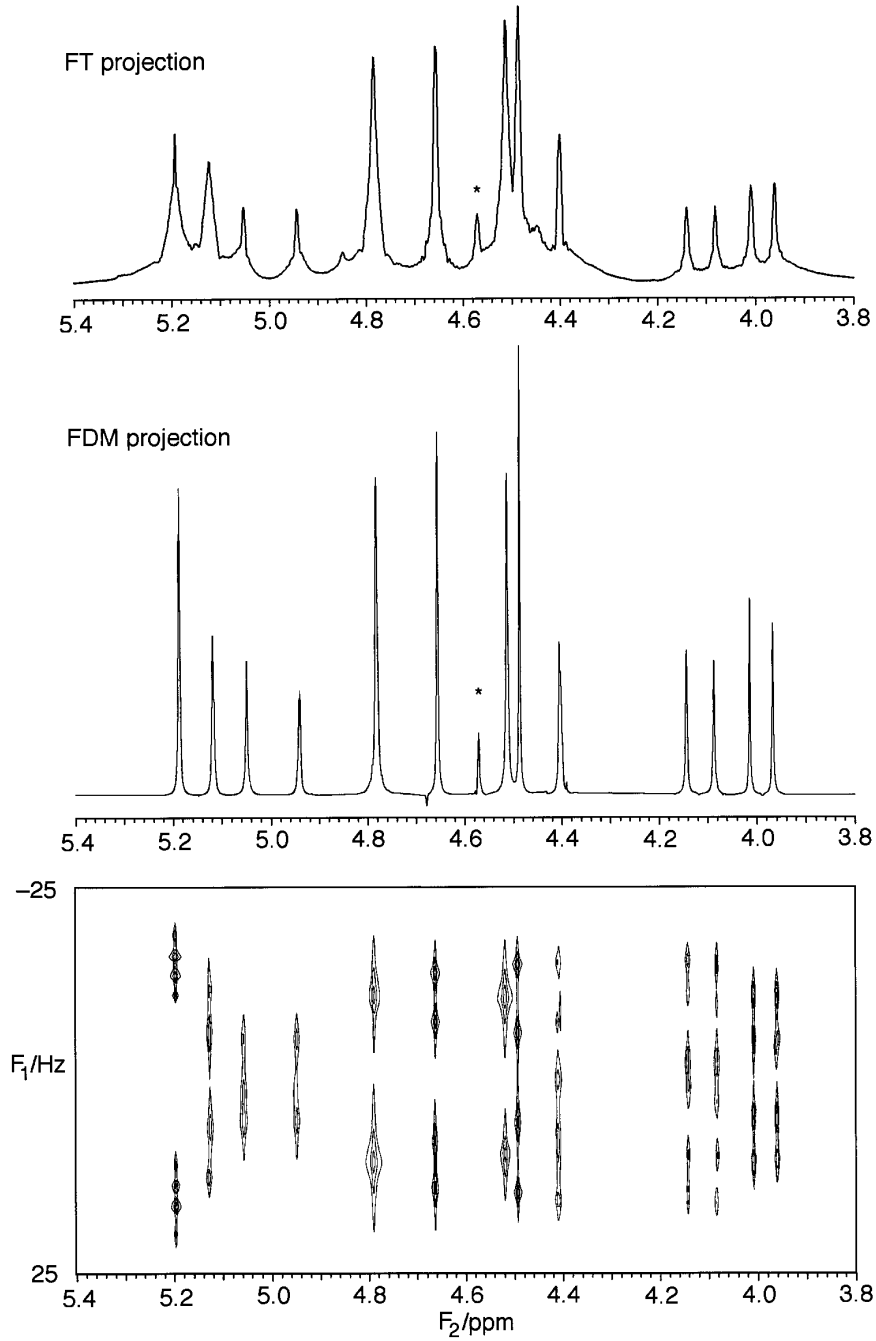

FIG. 4. (Top) Integral 45° projection of the absolute-value 2DFT *J* spectrum to obtain a proton-decoupled proton spectrum. A total of 64 t_1 increments were used, leading to a frequency-domain data matrix of 16K × 128 points over a spectral range of 10 kHz × 100 Hz after zero-filling. Dispersion-mode tails of the phase-twist lineshape lead to poor resolution in the projection. The asterisk marks an ''artifact'' arising from non-first-order coupling. (Center) The integral 45° projection of the absorption-mode ersatz spectrum constructed from the poles isolated by FDM. Only 16 t_1 increments were used. There is a dramatic improvement in resolution. (Bottom) An expanded portion of the ersatz 2D *J*-resolved spectrum after the transformation Eq. [9] has been applied to each pole. The original spectral width in F_1 was ±50 Hz, of which the central ±25-Hz region has been extracted. The FT spectrum (without zero-filling) would thus contain only 8 data points across this frequency range based on the same 16-point interferograms. Nevertheless, beautiful multiplet cross sections are obtained by FDM, without the baseline distortion characteristic of the usual phase-sensitive cross sections in the FT spectrum. The strong-coupling artifact lies outside the region shown.

jection, require a very high-resolution high signal-to-noise data matrix to work, do not handle lines of different width properly, falter if a line is narrower than presumed by the operator processing the data, and do not necessarily converge (*33*). ''Skyline projection'' distorts signal amplitudes and amplifies noise in the projection (*34*).

The second trace shows the absorption-mode projection from the 2D FDM (*7*) ersatz spectrum with the same data *but using only the first 16* t_1 *increments*, obtained as follows. The 2D time-domain signal was analyzed in the frequency region of interest and the poles (ω_{1k}, ω_{2k}) and amplitudes d_k were isolated. The absorption-mode spectrum was then constructed by Eq. [6]. Finally, a simple transformation of each pole

$$A(F_2) = -\sum_k \mathrm{Im}\left\{\frac{d_k}{2\pi F_2 + \mathrm{Re}\{\omega_{1k}\} - \omega_{2k}}\right\} \qquad [9]$$

was used to pick up each 2D peak literally and place it in the appropriate registration for the projection along F_1. There is clearly a dramatic improvement in resolution in the projected spectrum. This result is even more remarkable when the 6.25-Hz digital resolution in F_1 is taken into account. The ersatz absorption-mode 2D *J*-resolved spectrum at the bottom of Fig. 4 shows that the multiplet features are correctly identified even though many of the splittings are substantially less than 6 Hz. We are quite confident that, using 2D FDM, similar quality results could be obtained with even shorter time signals in each dimension, but we made no attempt to optimize the exact signal size. The entire 2D processing occupied an SGI workstation (200-MHz R4400 FPU) for less than half an hour.

SUMMARY

In summary, we have demonstrated a powerful new alternative to conventional methods of spectral analysis, the filter diagonalization method, and applied it to phase-sensitive 1D and 2D NMR spectra. Using FDM we were able to overcome the phase-twist lineshape problem, circumvent the strict limitations of the time-frequency uncertainty principle, and construct a 2D spectrum from a large data set in which no FT processing was used at all. It should be obvious that any phase-modulated data set of sufficient signal quality can be advantageously processed by FDM, and that the gains in higher-dimensional spectra may be even more noteworthy. More experimental work is clearly indicated, but FDM appears to be a fairly conservative data processing method that does not, for example, introduce spurious splittings. Our formulation of FDM is less subjective in application and interpretation than typical LP methods, as typical adjustable parameters like the filter length do not exist for FDM; it is also more efficient computationally. While we have compared *spectra* to show FDM versus the familiar FT method, when it comes to extracting *information* on line positions, widths, and intensities, FDM will prove to be of particular advantage versus spectral-based schemes, providing a database that can be used directly for the assignment procedure. Finally, while FDM is slower computationally than a simple FFT, it *scales* in much the same way, making it a compelling solution for very large multidimensional NMR data sets where other linear algebraic approaches become prohibitively expensive.

ACKNOWLEDGMENTS

This material is based on work partially supported by a Dreyfus Foundation Teacher–Scholar Award and by the National Science Foundation (CHE-9625674). H.S.T. was supported by the Petroleum Research Fund. The authors thank Mr. Jared Shaw for the loan and NMR assignment of compound **1,** and are indebted to Professor Benny Gerber for the use of the SGI workstation, and to Professor Christopher Grayce for the use of the Pentium 133 PC.

REFERENCES

1. R. R. Ernst, G. Bodenhausen, and A. Wokaun, ''Principles of Nuclear Magnetic Resonance in One and Two Dimensions,'' Clarendon Press, Oxford (1987).
2. G. Bodenhausen, R. Freeman, R. Niedermeyer, and D. L. Turner, Double Fourier transformation in high-resolution NMR, *J. Magn. Reson.* **26,** 133–164 (1977).
3. W. P. Aue, J. Karhan, and R. R. Ernst, Homonuclear broad band decoupling and two-dimensional *J*-resolved NMR spectroscopy, *J. Chem. Phys.* **64,** 4226–4227 (1976).
4. M. R. Wall and D. Neuhauser, Extraction, through filter-diagonalization, of general quantum eigenvalues or classical normal mode frequencies from a small number of residues or a short-time segment of a signal. I. Theory and application to a quantum-dynamics model, *J. Chem. Phys.* **102,** 8011–8022 (1995).
5. V. A. Mandelshtam and H. S. Taylor, Spectral analysis of time correlation function for a dissipative dynamical system using filter diagonalization: Application to calculation of unimolecular decay rates, *Phys. Rev. Lett.* **78,** 3274–3277 (1997).
6. V. A. Mandelshtam and H. S. Taylor, Harmonic inversion of time signals and its applications, *J. Chem. Phys.* **107,** 6756–6769 (1997).
7. V. A. Mandelshtam and H. S. Taylor, Multi-dimensional harmonic inversion by filter diagonalization, *J. Chem. Phys.,* in press.
8. V. A. Mandelshtam, H. Hu, and A. J. Shaka, Two-dimensional HSQC NMR spectra obtained using a self-compensating double pulsed field gradient and processed using the filter diagonalization method, *Magn. Reson. Chem.,* in press.
9. J. W. Pang, D. Neuhauser, and N. Moiseyev, Photoabsorption probability for a system governed by a time-dependent Hamiltonian through the (*t*, *t*′) formalism, *J. Chem. Phys.* **106,** 6839–6847 (1997).
10. T. P. Grozdanov, L. Andric, C. Manescu, and R. McCarroll, Discrete variable representation for highly excited states of hydrogen atoms in magnetic fields, *Phys. Rev. A* **56,** 1865–1871 (1997).
11. E. Narevicius, D. Neuhauser, H. J. Korsch, and N. Moiseyev, Resonances from short time complex-scaled cross-correlation probability amplitudes by the filter-diagonalization method, *Chem. Phys. Lett.* **276,** 250–254 (1997).
12. J. W. Pang and D. Neuhauser, Application of generalized filter-

diagonalization to extract instantaneous normal modes, *Chem. Phys. Lett.* **252,** 173–180 (1996).

13. P. Jungwirth, B. Schmidt, and N. Moiseyev, Vibrationally resolved spectra from short-time quantum molecular dynamics by the filter-diagonalization method, *Chem. Phys. Lett.* **280,** 177–184 (1997).
14. H. Hu, Q. N. Van, V. A. Mandelshtam, and A. J. Shaka, Reference deconvolution, phase correction and line listing of NMR spectra by the 1D filter diagonalization method, submitted for publication.
15. G. R. B. Prony, *J. Ec. Polytech. (Paris)* **1,** 22 (1795).
16. S. Marple, Jr., ''Digital Spectral Analysis with Applications,'' Prentice–Hall, Englewood Cliffs, NJ (1987).
17. R. Roy, B. G. Sumpter, G. A. Pfeffer, S. K. Gray, and D. W. Noid, Novel methods for spectral analysis, *Comput. Phys. Rep.* **205,** 109–152 (1991).
18. H. Barkhuijsen, R. de Beer, W. M. M. J. Bovée, and D. van Ormondt, Retrieval of frequencies, amplitudes, damping factors, and phases from time-domain signals using a linear least-squares procedure, *J. Magn. Reson.* **61,** 465–481 (1985).
19. J. Tang and J. R. Norris, LPZ spectral analysis using linear prediction and the *z*-transform, *J. Chem. Phys.* **84,** 5210–5211 (1986).
20. H. Gesmar and J. J. Led, Spectral estimation of complex time-domain NMR signals by linear prediction, *J. Magn. Reson.* **76,** 183–192 (1988).
21. D. S. Stephenson, Linear prediction and maximum entropy methods in NMR spectroscopy, *Prog. NMR Spectrosc.* **20,** 515–626 (1988).
22. G. Zhu and A. Bax, Improved linear prediction for truncated signals of known phase, *J. Magn. Reson.* **90,** 405–410 (1990).
23. R. de Beer and D. van Ormondt, Analysis of NMR data using time domain fitting procedures, *NMR Basic Prin. Prog.* **26,** 201–248 (1992).
24. H. Gesmar and P. C. Hansen, Fast linear prediction and its application to NMR spectroscopy, *J. Magn. Reson. A* **106,** 236–240 (1994).
25. Y.-Y. Lin, P. Hodgkinson, M. Ernst, and A. Pines, A novel detection-estimation scheme for noisy NMR signals: Applications to delayed acquisition data, *J. Magn. Reson.* **128,** 30–41 (1997).
26. J. C. Hoch and A. S. Stern, ''NMR Data Processing,'' Wiley–Liss, New York (1996).
27. G. A. Zhu and A. Bax, Two-dimensional linear prediction for signals truncated in both dimensions, *J. Magn. Reson.* **98,** 192–199 (1992).
28. H. Gesmar and J. J. Led, Two-dimensional linear-prediction NMR spectroscopy, *J. Magn. Reson.* **83,** 53–64 (1989).
29. H. Gesmar and J. J. Led, The application of the linear prediction principle to NMR spectroscopy, *in* ''Computational Aspects of the Study of Biological Macromolecules by Nuclear Magnetic Resonance Spectroscopy'' (J. C. Hoch, F. M. Poulson, and C. Redfield, Eds.), pp. 67–85, Plenum Press, New York (1991).
30. J. Tang and J. Norris, LP-ZOOM, a linear prediction method for local spectral analysis of NMR signals, *J. Magn. Reson.* **79,** 190–196 (1988).
31. M. H. Levitt and R. Freeman, Compensation for pulse imperfections in NMR spin-echo experiments, *J. Magn. Reson.* **43,** 65–80 (1981).
32. A. Bax, R. Freeman, and G. A. Morris, A simple method for suppressing dispersion-mode contributions in NMR spectra: The ''pseudo echo,'' *J. Magn. Reson.* **43,** 333–338 (1981).
33. A. J. Shaka, J. Keeler, and R. Freeman, Separation of chemical shifts and spin coupling in proton NMR. Elimination of dispersion signals from two-dimensional spectra, *J. Magn. Reson.* **56,** 294–313 (1984).
34. B. Blümich and D. Ziessow, Skyline projections in two-dimensional NMR spectroscopy, *J. Magn. Reson.* **49,** 151–154 (1982).